JOURNAL OF MATERIALS SCIENCE 11 (1976) 670–676

The effect of internal stresses on the yielding of case-hardened materials

J. L. PHILLIPS
C.E.G.B., Scientific Services Department, Portishead, Bristol, UK
J. W. MARTIN
Department of Metallurgy and Science of Materials, Oxford University, UK

The plastic yield behaviour has been studied as a function of case depth and of test temperature in three case-hardened materials: an internally oxidized copper alloy, an air-hardened titanium alloy and a nitrided steel. In the absence of any residual stresses, the yield stress of a material will rise in the presence of a hard case, and it is suggested that the effect of such residual stresses upon yielding may be predicted by employing a Hill criterion. A macroscopic model is developed on this basis which can account for the lowering of the tensile yield stress in the presence of a case in the nitrided steel and in the titanium alloy, and it is concluded that no effects due to internal stresses are present in internally oxidized copper–beryllium specimens.

1. Introduction
Although case-hardening is a widely used technique for improving the surface properties of metals, relatively little attention has been given to the effect that such cases may have upon the deformation and fracture behaviour of the treated materials under tensile stress, although the authors [1, 2] have examined these parameters in surface-hardened steel and titanium alloys. The present paper considers the possible contributions to the observed yield stress of case-hardened specimens.

The observed yield stress may be considered to be derived from several terms, namely the yield stress of the material in the absence of a case plus (a) a component arising from the volume fraction of the (hard) case (a "law of mixtures" contribution, which is often in practice very small), (b) a component arising from image forces on dislocations due to the case/core interface and (c) a component resulting from residual stresses at the case/core interface.

The principal theoretical studies on the third of the above factors have been carried out by Ebert *et al.* [3, 4], whose work originated from some fundamental studies of the stress state at the interface of a fibre-strengthened composite: they considered that a case-hardened cylindrical specimen may be regarded mathematically as a particular case of a fibre-composite material containing a single fibre in a thin matrix (i.e. the core of the case-hardened material is equivalent to the single fibre and the case of the material to the matrix of the composite).

In the work described below the plastic yield behaviour has been studied as a function of case depth and of test temperature in three case-hardened materials – in two of these internal stresses are significant, but they are absent in the third. A theory of yielding of case-hardened materials is developed, using the results of Ebert *et al.*, and the experimental data are interpreted in terms of the theory.

2. Experimental methods and results
Three case-hardened alloys possessing different crystal structures have been studied: an internally oxidized copper alloy, an air-hardened titanium alloy and a nitrided steel.

2.1. Testing methods
All mechanical tests were carried out on an Instron Universal Testing Machine; tensile test-pieces were

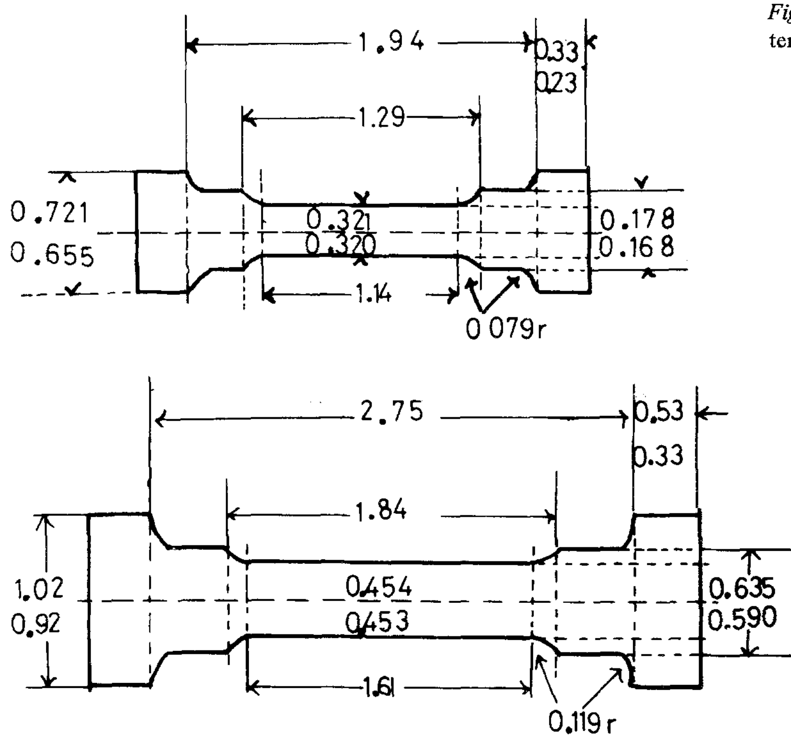

Figure 1 The dimensions (cm) of the tensile test-pieces.

machined to the size and shape shown in Fig. 1. Size (a) had to be used for the Ti and the Cu alloys because of the size of stock available, size (b) being used for the steel specimens. Cylindrical compression specimens were machined in each material such that their nominal diameters (d) were equal to those of the corresponding tensile specimens, and with lengths $3d$.

Tensile testing took place between 77 and 823 K. The lower range of temperature was achieved by means of a crystostatic bath and the higher range by using a small nichrome furnace. Compression testing took place between platens with WC anvils within a temperature range of 293 to 473 K, using a heated air supply.

2.2. Case hardening

2.2.1 Copper–beryllium

Composition

	Be	Sn	Fe	Ni	Zn	Cu
wt%	0.35	<0.01	<0.01	<0.01	<0.01	remainder

all other impurities <0.001%.

Test pieces were annealed and then internally oxidized at 1000 K by the Rhines "pack" method [5]. Two case depths were studied, corresponding to oxidation times of 21 and 65 min, respectively.

2.2.2. Ti–Al–Zr alloy

Nominal composition

	Al	Zr	W	Si	Ti
wt%	6	5	1	0.3	remainder

The alloy was solution-treated at 1323 K, and air-cooled. The structure was predominantly α, the weakly β-stabilizing W being held mainly in solution in the α-phase. The test pieces were case-hardened by heating in air for 100 hr at 823 K.

2.2.3. En 41b steel

Composition:

	C	Si	S	P	Mn	Ni	Cr	Mo	Al
wt%	0.42	0.38	0.013	0.015	0.57	0.19	1.56	0.17	1.01

Since differing nitriding times were involved, in order that the core of each test-piece had an identical thermal history, the following scheme of heat-treatment was followed, for a nitriding period of X h.

After annealing for $\frac{1}{2}$h at 1323 K and for $(50 - X)$h at 800 K the test-pieces were cleaned and surface polished. The specimens were then case-hardened by ion-discharge nitriding for X h at 800 K. This procedure was followed choosing values of X such that case-depths ranging from 4 to 140 μm were obtained.

In each material the depth of the case was determined by microhardness measurements across a polished section.

2.3. Experimental results

2.3.1. Cu–Be

Fig. 2 shows the variation of the 0.2% proof stress with temperature. It is seen that the presence of a case raised the proof stress at all temperatures tested; at constant temperature the incremental increase in proof stress rises as the case depth increases. It is also apparent that for a particular case depth at a given temperature, the numerical values of the compressive and tensile 0.2% proof stresses are identical.

2.3.2. Ti–Al–Zr

Fig. 3 shows the variation of the 0.2% proof stress with temperature. It is seen that the presence of a case lowers the tensile proof stress but raises the compressive proof stress at any given temperature within the range tested.

2.3.3. En 41b steel

Fig. 4 shows the variation in 0.2% proof stress with temperature. At low temperatures the presence of a case raises the proof stress, but for thin cases at temperatures between 373 and 523 K the proof stress of a case-hardened test piece may fall below that of a case-free specimen.

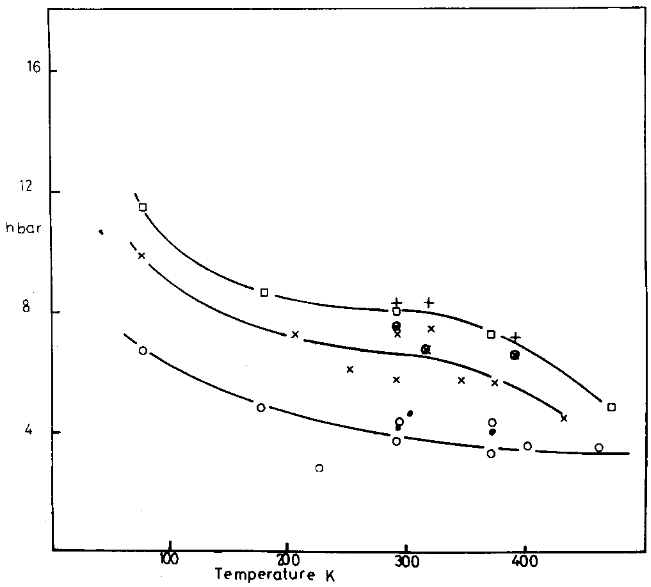

Figure 2 Variation of 0.2% proof stress with temperature for Cu–Be. Case-free specimens: ○, tensile; •, compression. 30 μm case: x, tensile; ⊗, compression. 55 μm case: □, tensile; +, compression.

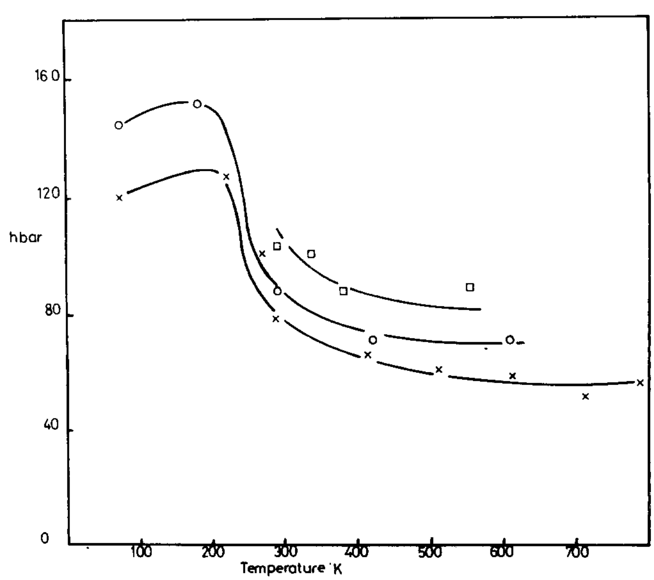

Figure 3 Variation of 0.2% proof stress with temperature for Ti–Al–Zr. Case-free specimens: ○, tensile. 25 μm case: x, tensile; □, compression.

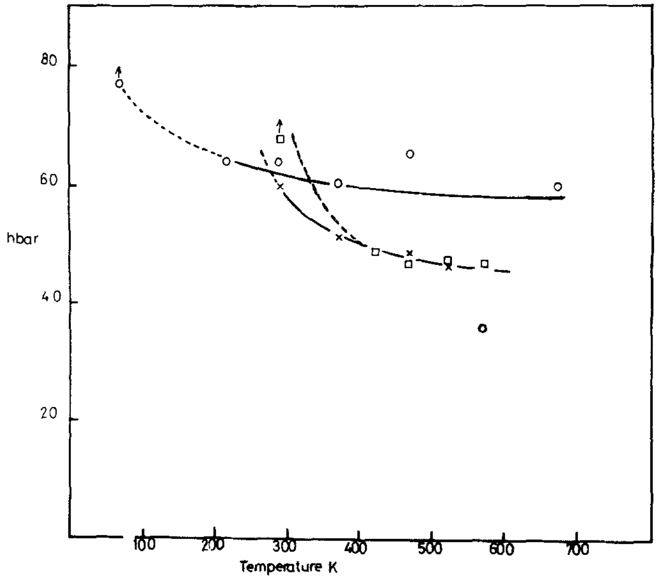

Figure 4 Variation of 0.2% proof stress with temperature for En 41b steel. Case-free specimens: ○, tensile. 4 μm case: x, tensile. 16 μm case: □, tensile.

3. Discussion

In general, the formation of a hard surface case on a specimen by a diffusion heat-treatment, may, at the same time, involve the development of a system of internal stresses which will play an important role in determining the yield stress of the specimen.

3.1. Yield stress of a case-hardened cylinder containint residual stresses

The logical starting-point for a general theory of yield for such a solid is the use of the Hill [6] criterion for plastic flow, which is an extension of the more well-known Von-Mises equation. In order to make the complex mathematics amenable to physical interpretation a number of assumptions will be made, as follows:

(i) Yielding is initiated at, or near to the case/core interface. This is in agreement with the results of Ebert and Gadd [3] and of Mihelich [7].

(ii) The magnitude of the residual radial stress at the case/core interface is negligible compared with those of the tangential and longitudinal residual stresses. This is certainly true for the results of Linhart [8] on nitrided steels, but the assumption will have little effect upon the yield surface other than producing a shift of the origin of the axes: for a cylinder whose axis is along z this shift would be along the line $y = x$ and if necessary this could be taken into account in computations.

(iii) When an external stress is applied parallel to z we assume again that the magnitude of the

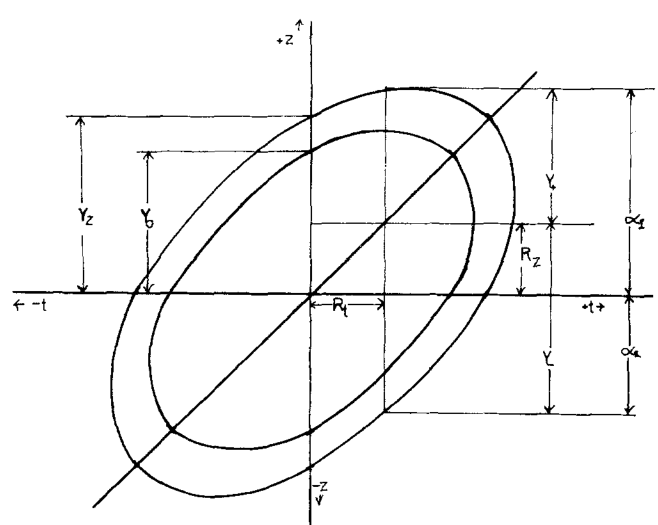

Figure 5 Biaxial yield surface for case-hardened material illustrating initiation of plastic flow.

residual radial stress is negligible, in comparison with it.

(iv) We will define uniaxial yield stresses for the material in the axial (z) and tangential (t) directions as Y_z and Y_t; in general $Y_z \neq Y_t$.

We may now construct a biaxial yield surface (Fig. 5); the inner ellipse represents the yield behaviour of the material in the absence of residual stresses (i.e. of uniaxial yield stresses Y_0) and the outer ellipse represents the yield surface when axial and tangential residual stresses (R_z and R_t respectively) are present. In this situation the tensile and compressive yield stresses of the case-hardened specimen are Y_+ (defined as a positive stress) and Y_- (a negative stress) respectively, when the test piece is deformed parallel to the z axis.

We may assume this yield surface is described by an equation of the form

$$ax^2 + by^2 + cxy + dx + ey + f = 0 \quad (1)$$

(using the notation $\sigma_z \rightarrow y, \sigma_y \rightarrow x$).
This closed surface must pass through the points $(-Y_t, 0)$, $(-Y_t, -Y_z)$, $(0, -Y_z)$, $(Y_t, 0)$, (Y_t, Y_z), $(0, Y_t)$, so that Equation 1 becomes

$$\frac{y^2}{Y_z^2} + \frac{x^2}{Y_t^2} - \frac{xy}{Y_z Y_t} = 1. \quad (2)$$

In order to evaluate Y_+ and Y_- in terms of Y_z and Y_t and the residual stresses R_z (axial) and R_t (tangential) in the case we rewrite Equation 2

$$\frac{y^2}{Y_z^2} + y\left(\frac{R_t}{Y_t Y_z}\right) + \left(\frac{R_t^2}{Y_t^2} - 1\right) = 0. \quad (3)$$

This is a quadratic equation in y with roots α_1 and α_2 ($\alpha_1 > \alpha_2$). From Fig. 5 it is easily shown that

$$\begin{aligned} Y_+ + R_z &= \alpha_1 \\ Y_- - R_z &= \alpha_2. \end{aligned} \quad (4)$$

Now solving Equation 3 and taking the positive square root we obtain

$$\begin{aligned} \alpha_1 &= \frac{R_t Y_z}{2Y_t} + \frac{Y_z}{2}\left(4 - \frac{3R_t^2}{Y_t^2}\right)^{\frac{1}{2}} \\ \alpha_2 &= \frac{R_t Y_z}{2Y_t} - \frac{Y_z}{2}\left(4 - \frac{3R_t^2}{Y_t^2}\right)^{\frac{1}{2}} \end{aligned} \quad (5)$$

From Equation 4 the following relationships may be derived:

$$\begin{aligned} Y_+ &= \frac{R_t Y_z}{2Y_t} + \frac{Y_z}{2}\left(4 - \frac{3R_t^2}{Y_t^2}\right)^{\frac{1}{2}} - R_z \\ Y_- &= \frac{R_t Y_z}{2Y_t} - \frac{Y_z}{2}\left(4 - \frac{3R_t^2}{Y_t^2}\right)^{\frac{1}{2}} - R_z. \end{aligned} \quad (6)$$

Since these equations for Y_+ and Y_- contain four unknown quantities, in order to test the theory we will firstly make the approximation that

$$Y_t = Y_z = Y,$$

which gives

$$\begin{aligned} Y_+ &= \frac{R_t}{2} - R_z + \left(Y^2 - \frac{3}{4}R_t^2\right)^{\frac{1}{2}} \\ Y_- &= \frac{R_t}{2} - R_z - \left(Y^2 - \frac{3}{4}R_t^2\right)^{\frac{1}{2}}. \end{aligned} \quad (7)$$

We will now derive a relationship of the form

$$R_t = f(R_z),$$

and here the analysis due to Ebert and Gadd [3] can be utilized to investigate the distribution of residual stresses in the composite due to the case-strain (γ) arising from the case-hardening operation. Since the elastic constants of both core and case will be virtually identical, the Ebert-Gadd analysis can be simplified leading to the following relationships:
For the case:

$$\begin{aligned} R_z &= \frac{E(1+\gamma)}{(1-\gamma)}; \\ R_r &= -\frac{E(1+\gamma)}{2(1-\gamma)}\left(\frac{b^2}{r^2} - 1\right) \\ R_t &= \frac{E(1+\gamma)}{2(1-\gamma)}\left(\frac{b^2}{r^2} + 1\right) \end{aligned} \quad (8)$$

where E = Young's modulus, b = radius of specimen, r = radial vector in cylindrical co-ordinates; and for the core, (Poisson ratio = ν, radius a)

$$\begin{aligned} R_z &= -\frac{2\nu E(1+\gamma)}{(1-\gamma)} \cdot \frac{(b-a)}{b} \\ R_r &= -\frac{E(1+\gamma)}{(1-\gamma)} \cdot \frac{(b-a)}{b} = R_t. \end{aligned} \quad (9)$$

Since the ratio $(b-a)/b$ is very small, all residual stresses in the core are negligible, and also (from

Equation 9) are seen to be independent of radius.

It follows from Equation 8 $R_z/R_t = -1$ at the case/core interface. Thus we may write the interfacial residual stress as R and substitute in Equation 6 to give

$$Y_+ = -R/2 + (Y^2 - \tfrac{3}{4}R^2)^{\frac{1}{2}}$$
$$Y_- = -R/2 - (Y^2 - \tfrac{3}{4}R^2)^{\frac{1}{2}} \qquad (10)$$

and solving for R and Y we obtain:

$$R = -(Y_+ + Y_-)$$
$$Y^2 = Y_+^2 + Y_-^2 + Y_- Y_+ \qquad (11)$$
$$= R^2 - Y_- Y_+.$$

3.2. Interpretation of experimental data

3.2.1. Cu–Be

It is very clear from the results of Fig. 2 that the presence of a case raises the yield stress at all temperatures tested. Since tensile and compressive yield stresses are identical, from Equation 11 it may be concluded that residual stresses do not play any part in the raising of the proof stress in the internally oxidized material. There is indeed no theoretical or experimental evidence to suggest that extensive residual stresses are present in internally oxidized Cu–Be.

Mahajan and Himmel [9] studied the flow stress of Ag case-hardened by internal oxidation, and claimed that the observed flow stress can be calculated by a "method of mixtures" calculation. For this explanation to be true in the present system, the necessary proof stress of the case would have to be of the order of 100 hbar, i.e. at least twenty times that of the case-free material. A typical value for the ratio of the 0.2% proof stresss of internally oxidized Cu–Be to that of unoxidized Cu–Be is about seven. Careful examination of Mahajan and Himmel's data suggests that the observed flow stress is in general substantially greater than the calculated flow stress, and it is suggested that in that work, as in the present system the increase in proof stress arises partially from some form of dislocation interaction at the case-core interface. This phenomenon has been studied by (e.g.) Greenfield and his coworkers [10] using single crystal specimens with surface diffusion layers upon them, and it will not be elaborated upon here.

3.2.2. Ti–Al–Zr

The effect of the case upon the proof stress of this alloy can be conveniently studied by means of the theory developed in Section 3.1 above. By use of Equation 11 it is possible to calculate from the test data: R, a measure of the residual stresses present, ΔY, the increase in specimen yield stress due to the case in the absence of residual stresses. The results are shown in Table I.

At temperatures below 400 K it is seen that $\Delta Y/Y_0$ has a comparatively low value. In the region of room temperature dislocation mobility is limited, but the increasing effect of the case with increasing temperature may be explained by the increasing dislocation mobility, which increases the bulk effect of the case.

As the temperature increases above 400 K the further increase in dislocation mobility will enable any atomistic barriers set up by the case to be overcome with increasing ease (whatever the form these barriers may take), so that in this range the behaviour of the $\Delta Y/Y_0$ versus temperature is similar to that of the internally oxidized Cu–Be material.

3.2.3. En 4lb steel

The analysis of the 0.2% proof stress data may be handled in a similar way to that of the Ti–Al–Zr alloy. From Equation 11 together with some compressive yield stress data it is possible to calculate R, the residual stresses present and $\Delta Y/Y_0$ the fractional change in yield stress due to the case in the absence of any residual stresses. These results are shown in Table II for specimens with case

TABLE I Yield stress data and calculated residual stresses in Ti–Al–Zr

T (K)	Y_0 (hbar)	Y_+ (hbar)	Y_- (hbar)	R (hbar)	Y (hbar)	$\Delta Y = Y - Y_0$ (hbar)	$\Delta Y/Y_0$ (%)
293	87.5	77.5	−103	+25.5	92.9	5.40	6.24
350	79.5	70.5	−95	+24.5	84.4	4.90	6.16
400	72.5	66.5	−89	+23.5	80.4	7.90	10.90
450	70.5	64.5	−85	+21.5	77.1	6.60	9.45
500	70.0	63.0	−84	+21.0	75.8	5.80	8.29
550	70.0	61.5	−83	+21.5	74.6	4.60	6.57

TABLE II Yield stress data and calculated residual stresses in En 4lb steel

Case depth (μm)	Test temp. (K)	Y_0 (hbar)	Y_+ (hbar)	Y_- (hbar)	R (hbar)	Y (hbar)	ΔY (hbar)	$\Delta Y/Y_0$ (%)
4	293	64	60	−82	22	73.5	13.5	+21
4	418	59	50	−65	15	59	0	0
16	293	64	65	−88	23	79	15	+23
16	418	59	49	−66	17	59	0	0

depths of 4 and 16 μm. All specimens with thicker cases showed no evidence of yielding at all temperatures.

Our theoretical derivation of a model for residual stress (Equation 9) indicates that R should not be a function of case depth, and the results of Table II bear out this suggestion.

From the limited amount of data available, it appears that the usual features of yielding arise, i.e. $\Delta Y/Y_0$ decreases with increasing temperature and decreasing case-depth, and it may be accounted for on the same basis as that given for the Cu–Be and for the Ti alloy above 400 K.

The proof stress results (Fig. 4) can now be interpreted: at low temperatures ($T < 300$ K) for all case depths, the yielding of the specimen is dictated by the large value of $\Delta Y/Y_0$. This term tends to raise the proof stress despite the effect of the residual stresses attempting to lower it.

At higher temperatures ($T > 300$ K) the value of $\Delta Y/Y_0$ is still critical for specimens with thick cases (case depth $> 16\,\mu$m), consequently this term dominates the deformation of thick-cased specimens. For specimens with thinner cases (4 and 16 μm) the value of $\Delta Y/Y_0$ is now extremely low and tending to zero, so the residual stress term R dominates the deformation and causes the proof stress to be lowered. Hence under these conditions for thin cases, $Y \simeq Y_0, R > 0$, and consequently $Y+ < Y_0$.

Since, as already stated, the magnitude of the residual stresses is independent of case depth, this hypothesis is supported by the fact that at temperatures near to 500 K the proof stresses for specimens with thin cases (4 and 16 μm) fall on a common curve. If we linearly extrapolate the value of R in Table II to 473 K, we obtain a value of 12 hbar. Thus if $Y = Y_0$, $Y+ = 53$ hbar; this agrees favourably with a value of 49 hbar obtained experimentally.

4. Conclusions

(1) In the absence of any residual stresses, the yield stress of a material will rise in the presence of a hard case.

(2) The effect of residual stresses may be superimposed upon the behaviour of (1) according to the Hill extension of the von-Mises criterion.

(3) The mechanism (2) can account for the lowering of the tensile yield stress in the presence of a case in En4lb steel and Ti–Al–Zr, but it is concluded that no effects due to internal stresses are present in internally oxidized Cu–Be specimens.

Acknowledgements

The authors acknowledge with gratitude the support of Messrs IMI Ltd and (JLP) the Science Research Council for the award of a research studentship during the tenure of which the work was carried out.

References

1. J. L. PHILLIPS and J. W. MARTIN, Proceedings of the International Conference on Titanium, Cambridge, Mass., 1972, (Plenum Press, New York, 1973) p. 2109.
2. *Idem*, Proceedings I.S.I. Conference "Physical Metallurgy Aspects of Surface Coatings", May 1973.
3. L. J. EBERT and J. D. GADD, "Fiber Composite Materials" (Amer. Soc. Metals, Cleveland, Ohio, 1964) p. 89.
4. L. J. EBERT, F. T. KROTINE and A. R. TROIANO, *Trans ASME Ser. D. (J. Basic Eng.)* 87 (1965) 871.
5. F. N. RHINES, W. A. JOHNSON and W. A. ANDERSON, *Trans Amer. Inst. Min. Metall. Engrs.* **147** (1942) 205.
6. R. HILL, "The Mathematical Theory of Plasticity" (Clarendon Press, Oxford, 1956).
7. J. L. MIHELICH, M.S. Thesis Case Inst. of Tech. (1961).
8. V. LINHART, Proceedings of the International Conference (Warsaw) on "Fatigue resistance of materials and metal structural parts" edited by A. Buck (Pergamon Press, Oxford, P.W.N. Warsaw, 1960).
9. S. MAHAJAN and L. HIMMEL, *Acta Met.* **20** (1972) 1313.
10. Y. G. NAKAGAWA and I. G. GREENFIELD, *ibid* **21** (1973) 367.

Received 26 August and accepted 3 October 1975.